11th Asia-Pacific Conference on Combustion,
The University of Sydney, NSW Australia
10th -14th December 2017.

Mode-Switching Behaviour of Preheated and Diluted Flames in a Stagnation Burner

Bin Jiang, Robert. L. Gordon, Mohsen. Talei

Department of Mechanical Engineering

University of Melbourne, Parkville, 3010, Australia

Abstract

The combustion mode of preheated and diluted methane/air flames is studied with a one-dimensional (1D) stagnation flame model. The species transport budget is used to determine the combustion mode between premixed flame propagation and autoignition. The autoignition delay time decreases with increasing the dilution level, pressure, oxygen concentration, or adding minor species. The combustion mode can then change from premixed flame propagation to autoignition. This behaviour agrees with previous studies on autoignition. Increasing the inlet velocity has been found to switch the combustion mode from premixed flame propagation to autoignition and back to premixed flame propagation. This double mode switch may be directly related to a competition between autoignition delay time and flame speed of premixed flames as well as features of diluted flames such as the weakened reaction zone.

1 Introduction

Environmental concerns and emissions regulation have motivated researchers to develop novel combustion techniques for achieving ultra-low emissions. Recently, Moderate or Intense Low oxygen Dilution (MILD) combustion has emerged as a promising solution to achieve ultra-low nitrogen oxides (NOx) and carbon monoxide (CO) as well as to maintain high thermal efficiency, fuel flexibility and low noise emission for gas turbines (GTs) [1]. Understanding MILD combustion has become an area of active research, such as the definition of MILD regime [2] and the distinction of combustion regimes in MILD-like combustion [3]. MILD combustion may be possible to be achieved in gas turbines by diluting fresh reactants with hot combustion products. This dilution can be established with internal recirculation or staged combustion. The FLameless OXidation COMbustion (FLOXCOM)[4], LEan Azimuthal Flame (LEAF) combustor [5] and Colorless Distributed Combustion (CDC) [6] use internal recirculation. FLameless OXidation (FLOX) [7] and the Alstom/GE GT24/26 [8] use staged combustion, although [8] does not operate in true MILD condition.

The combustion mode is important for the modelling of the combustion process. Combustion models for premixed flame propagation and autoignition have traditionally been developed for a single combustion mode and may not be suitable when the combustion system can feature different modes.

Mode switching between premixed flame propagation and autoignition can affect flame stabilization, especially in terms of combustor stability and operating flexibility. For example, a premixed propagating flame will move downstream of the injection point, while an autoignition flame moves upstream of the injection point in a secondary stage of a staged GT combustor at elevated pressures [9].

The presence of a wall can introduce effects related to strain rate, heat loss and the boundary layer [10], which may affect the combustion mode. In MILD or staged combustion, the internal recirculation can stabilize the flame close to a wall. This is especially true for the jet in cross flow configuration in a staged combustor, which can induce flame-wall interaction under different momentum ratios of the jet and cross flow [11]. Furthermore, the reaction zone in MILD combustion is generally distributed, such that compared to traditional GT combustors the contact area of the flame and combustor wall may increase. Therefore, it is important to understand wall effects on preheated and diluted flames. The combustion mode of a stagnation flame is studied in this paper under different conditions relevant to a wall-bounded MILD GT combustor, drawing on the dilution method from Sidey et al. [12] and the transport budget from Gordon et al. [13].

2 Numerical Methods

The stagnation-flame reactor of CHEMKIN PRO [14] was used to simulate the effect of a wall on a steady, preheated and diluted flame. The computational domain was 2 cm long from the burner exit to the stagnation plate. The wall was considered to be inert with a constant temperature (300K). In order to ensure an accurate convergence and grid independent solution, the adaptive meshing criteria for both the largest relative gradient and curvature were 0.02.

Methane (CH_4) was used as the fuel with the gas-phase oxidation described by GRI 3.0 [15]. All simulations were performed with mixture-averaged transport properties, and with the Soret effect considered.

Dilution was achieved by mixing stoichiometric CH_4/air at 300K and combustion products at equilibrium temperature. The degree of mixing is defined by the "dilution level" ζ, which is the ratio of hot product mass flow rate to the fresh reactant mixture. The mixture temperature and oxygen (O_2) mole fraction at different dilution levels are shown in Fig. 1. The detailed dilution method can be found in our previous work [12]. To verify the numerical model, simulation results from Sidey et al. [12] were reproduced, showing good agreement [16].

Corresponding author.
E-mail address:jiangb1@student.unimelb.edu.au

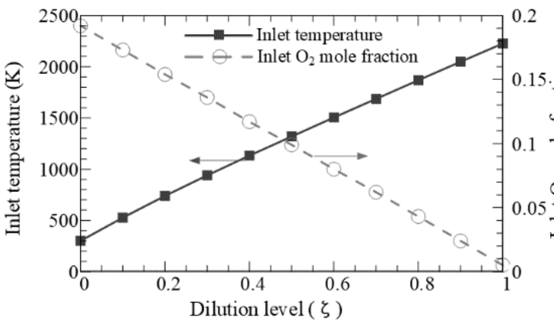

Figure 1: Mixture temperature and O_2 molar fraction profiles under different dilution levels.

3 Indicator for Combustion Modes

The species transport budget is used in this paper to identify the combustion mode [13]. In an autoignition flame, the mass diffusion in the reaction zone is relatively smaller than the mass convection and reaction. However, the amount of mass diffusion in a premixed flame is significant in both the preheat and reaction zones. The transport budget is calculated based on the steady-state species conservation equation given by:

$$-\rho u \frac{dY_k}{dx} - \frac{d}{dx}(\rho Y_k V_k) + W_k \dot{\omega}_k = 0 \tag{1}$$

The first term on the left-hand side (LHS) of the equation represents the mass convection (C), which is the summation of mass convection in axial (x) and radial directions. The second term represents the molecular diffusion (D), and the third is the reaction term (R). Here, ρ is the mixture density, u is the axial velocity, Y_k is the mass fraction of a species k, W_k is the molecular weight of a species k, $\dot{\omega}_k$ is the net reaction rate of a species k, and V_k is the diffusion velocity given by:

$$V_k = -\frac{D_{km}}{X_k}\frac{dX_k}{dx} - \frac{D_k^T}{\rho Y_k}\frac{1}{T}\frac{dT}{dx} \tag{2}$$

where X_k is the mole fraction of a species k, D_{km} is the ordinary mixture-averaged diffusion coefficient, D_k^T is the thermal diffusion coefficient, T is the mixture temperature.

Equation (2) shows that there is a double derivative in the diffusion term, which magnifies any discretization and numerical noise. Hence, this term is smoothed by using the Robust LOcally regrESSion (RLOESS) method [17].

Figure 2(a) shows the OH transport budget of a conventional premixed flame at ζ=0. Significant mass diffusion in both the preheat and reaction zones are visible as marked with (1) and (2), respectively. Fig. 2(b) shows the OH transport budget of an autoignition flame at ζ =0.7 with negligible mass diffusion.

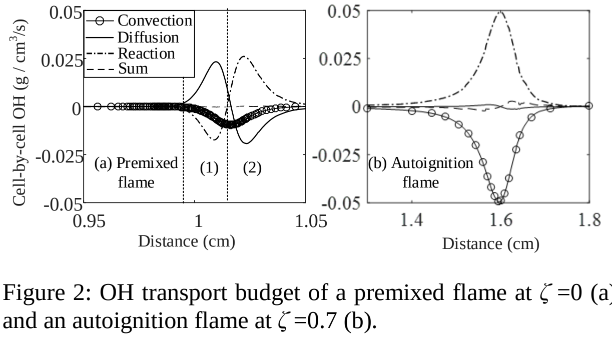

Figure 2: OH transport budget of a premixed flame at ζ =0 (a) and an autoignition flame at ζ =0.7 (b).

4 Results

4.1 Effects of Dilution

OH transport budgets of two dilution levels are presented in Fig. 3. At ζ =0.5, the flame is stabilized by the flame propagation indicated by the balance between mass diffusion and convection in the preheat zone. At ζ = 0, the mass diffusion in the preheat zone is nearly zero, indicating that the flame is stabilized as an autoignition flame. The mixture temperature increases with increasing dilution levels (Fig. 1), thus decreasing the autoignition delay time (Equation 3 [18]). Conversely, the decrease of oxygen concentration at a high dilution level should increase autoignition delay time. However, its effects on autoignition delay time appear to be smaller than the effect of mixture temperature.

$$t = 1.77 \times 10^{-14} \exp(18693 / T)[O_2]^{-1.05}[CH_4]^{0.66}[HC]^{-0.39} \tag{3}$$

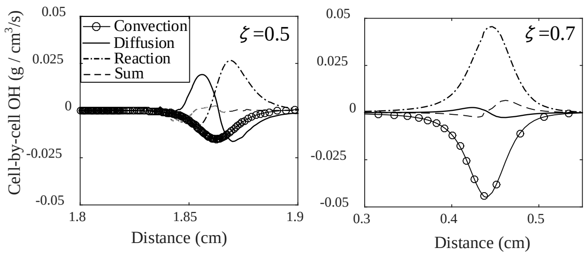

Figure 3: Dilution level (ζ) effects on the OH transport budget at an equivalence ratio (Φ)=1, inlet velocity (V_{in})=50m/s, combustor pressure (P)=1 atm.

With using the combustion products as the diluent, minor species in the products can affect the species transport budget. To study this, a simulation was conducted with only major combustion products as the diluent, i.e. CH_4, O_2, N_2, CO_2, H_2O, CO, H_2 and NO. Figure 4 shows that the combustion with all minor species in the diluent exhibits an autoignition mode, while the combustion with only major species is stabilized by premixed flame propagation. This result reflects that the minor species can reduce the autoignition delay time, which is consistent with the observations in Ref. [12].

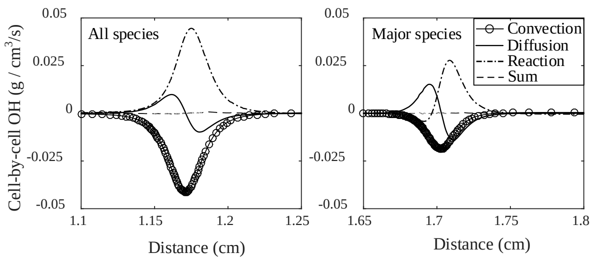

Figure 4: Effects of the minor species on OH transport budget at Φ=1, ζ=0.6, V_{in}=20m/s, P=1atm.

4.2 Effects of Combustor Pressure

Figure 5 shows that the diffusion term decreases with increasing pressure, which promotes the transition from a premixed flame to an autoignition flame. The main reason for the mode switching is that autoignition delay time decreases with increasing pressure as reported from the Ref. [19]. The flame moves upstream at elevated pressures, which agrees with Ref. [9].The peak value of the transport budget at a high pressure is nearly six times larger than at the low pressure, as the unburned flow velocity and density of upstream flame increases with pressure as reported in Ref. [9].

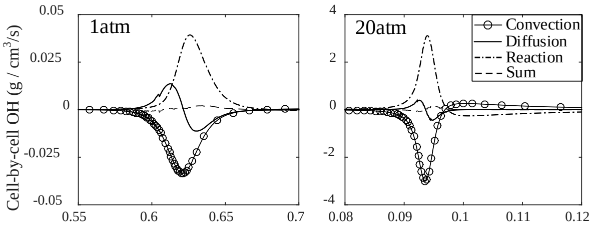

Figure 5: Effects of the pressure on OH transport budget at ζ =0.6, Φ=1, V_{in}=10m/s.

4.3 Effects of Oxygen Concentration

MILD combustion usually has oxygen concentrations from 3% to 12% [4], while in a conventional GT with lean premixed combustion, the O_2 mole fraction is around 15%. To eliminate the effects of other parameters, the diluent was set to be pure N_2, and the CH_4 mole fraction is fixed at 0.03. The compositions of reactants for the two different oxygen mole fraction cases are $CH_4/O_2/N_2$=0.03:0.06:0.91 at Φ=1 and $CH_4/O_2/N_2$= 0.03:0.2:0.77 at Φ =0.3. To clearly show the mode-switching behaviours for two different O_2 mole fractions, the mixture temperature was chosen to be 1400K. In the secondary combustor of a staged GT, the reactant can be preheated above 1000 ^oC, which is representative of staged combustion condition [8]. As seen in Fig. 6, the combustion mode switches from premixed flame propagation to autoignition with increasing oxygen concentration, since the autoignition delay time decreases with increasing the oxygen concentration, which agrees with the prediction of Equation (3). The peak of the reaction term at 0.06 O_2 mole fraction is two times smaller than the peak value with 0.2 O_2 mole fraction. The reaction zone is weakened by decreasing the O_2 mole fraction, which is consistent with Ref. [20].

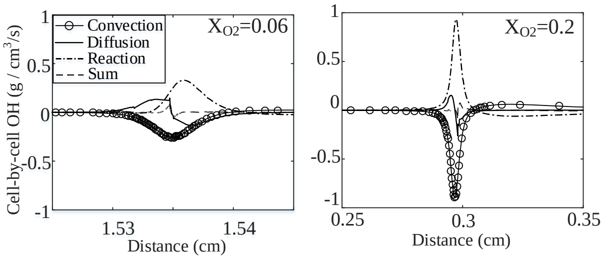

Figure 6: Effects of O_2 mole fraction on OH transport budget at mixture temperature (T_{in})=1400K, V_{in}=10m/s, P=10 atm.

4.4 Effects of Inlet Velocity

The inlet velocity is changed by varying the reactant mass flow rate. Below 20m/s inlet velocity, the mass transport in the preheat zone is balanced by mass diffusion and convection, and reaction is negligible as shown in Fig. 7. Therefore, the combustion is stabilized by premixed flame propagation. As the inlet velocity varies from 20m/s to 30m/s, the OH transport budget is balanced by mass convection and reaction with small contributions from mass diffusion, which indicates an autoignited combustion mode. At a high inlet velocity of 80m/s, the diffusion term again starts to dominate the preheat zone, and thereby the flame is understood to be stabilized by premixed flame propagation. As seen in Fig.7, unlike the other three inlet velocities, the OH transport budget at 80m/s inlet velocity has non-zero components near the wall. As the flame stabilises closer to the wall, a decreasing temperature induced by the wall heat transfer activates radical recombination reactions[10].

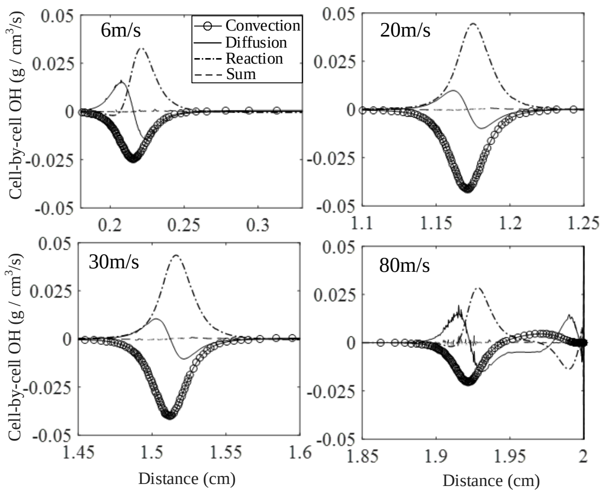

Figure 7: Effects of the inlet velocity on OH transport budget at Φ=1, ζ=0.6, P=1atm.

6 Discussion

With increasing dilution levels, combustor pressure and oxygen concentration, the combustion mode switches from premixed flame propagation to autoignition. This might be attributed to the competition between premixed flame propagation timescale and the autoignition delay time.

At ζ =0.6, increasing the inlet velocity switches the combustion mode from premixed propagation to autoignition and then back to premixed propagation. Figure 8 shows the variation of the burning velocity, defined as the gas velocity at the peak of heat release rate, as a function of inlet velocity [21]. With increasing the inlet velocity, the burning velocity increases almost linearly at low inlet velocities (below 12m/s) and reaches its maximum around 25m/s. After this point, the burning velocity decreases with increasing the inlet velocity.

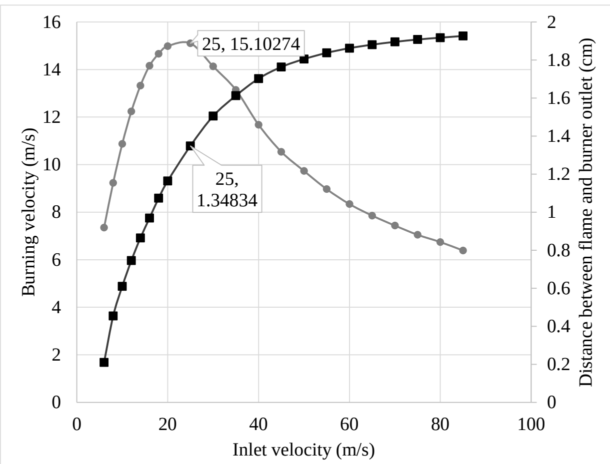

Figure 8: Evolution of flame burning velocity and flame position with increasing the inlet velocity at ζ =0.6, Φ=1, P=1atm.

Figure 8 shows that the flame front (measured from location of the peak heat release rate) is closer to the wall as the inlet velocity increases. At low inlet velocities, the burning velocity is a strong function of the inlet velocity, because the flame is still far from the cold wall. However, at some distances from the wall (around 22 unstretched flame thickness (0.3mm)), the flame appears to be affected by the presence of the wall, and the burning velocity features a decreasing trend.

Two important conclusions can be made from this observation. Firstly, the linear relationship between the burning velocity and the inlet velocity proposed in the previous study [21] does not hold for high values of inlet velocity. The second conclusion is related to the convection term in Equation 1. Figure 7 shows that the diffusion term features insignificant variation for different velocities, while the convection term is a strong function of the burning velocity as expected. Increasing the inlet velocity leads to the convection term dominating the diffusion term, promoting an autoigntion combustion mode. However, closer to the wall, the convection term becomes weaker again and therefore a premixed flame is established before extinction occurs.

Combustion-mode switching is also related to the competition of autoignition delay time and flame speed of premixed flames. Residence time increases with increasing flame-nozzle distance, while decreases with increasing inlet velocity. Figure 8 shows that increasing the inlet velocity increases the flame-nozzle distance but at decreasing rate due to increasing local strain rates. Therefore, at intermediate inlet velocities (20m/s to 30m/s), the residence time can approach the autoignition delay time.

Combustion-mode switching is an important feature of diluted flames that can have significant implications for modelling. Compared with conventional flames, the reaction zone of preheated and diluted flames is generally weaker due to low oxygen concentrations, such that stretch may have a stronger effect on the reaction zone. Therefore, linear models in the stretched flame theory may not capture the behaviour correctly.

7 Conclusion

Combustion modes of preheated and diluted flames have been investigated using the CHEMKIN stagnation burner geometry. The species transport budget is used to identify changes in the combustion mode induced by varying the inlet velocity, dilution level, diluent composition, combustor pressure and oxygen concentration. Increasing dilution level, pressure and oxygen concentration, and adding minor species in the diluent promotes autoignition, which is consistent with previous studies. With increasing the inlet velocity, the combustion mode switches from premixed flame propagation to autoignition, and can change back to premixed flame propagation. This double mode switching correlates with changes in the burning velocity, which can affect the relative magnitudes of diffusion and convection terms in the species transport budget. Changes in the strain rate may also affect the timescale competition. In the future, transient models will be used to study the temporal evolution of combustion mode, as well as the response of the combustion mode to changes in the local properties of diluted flames, such as weakened reaction zones.

8 Acknowledgment

Bin Jiang acknowledges the financial support of the China Scholarship Council. Robert Gordon receives support from the Royal Academy of Engineering as a Newton International Fellowship Alumnos.

References

[1]. A. Cavaliere, M. de Joannon, Prog. Energy Combust. Sci. 30 (4) (2004) 329-366.

[2]. M.J. Evans, P.R. Medwell, H. Wu, A. Stagni, M. Ihme, Proc. Combust. Inst. 36 (3) (2016) 4297-4304.

[3]. O. Schulz, T. Jaravel, T. Poinsot, B. Cuenot, N. Noiray, Proc. Combust. Inst. 36 (2) (2017) 1637-1644.

[4]. G. A. Rao, Y. Levy, 8th HiTACG conference, Poznan (p. 13) (2010).

[5]. J.A.M. Sidey, I.E. Helou, R.L. Gordon, G. Bourque, E. Mastorakos, 11th International ERCOFTAC Symposium on Engineering Turbulence Modelling and Measurements. (2016).

[6]. A.E.E. Khalil, A.K. Gupta, Fuel. 195, 2017, 113-122.

[7]. T. Roediger, O. Lammel, M. Aigner, C. Beck, W. Krebs, J Eng Gas Turbine Power. 135 (3) (2013) 1-12.

[8]. D. Guyot, G. Tea, C. Appel, J Eng Gas Turbine Power. 138 (5) (2016) 051503.

[9]. P. Habisreuther, F.C.C. Galeazzo, C. Prathap, N. Zarzalis, Combust. Flame 160 (12) (2013) 2770-82.

[10]. F.N. Egolfopoulos, H. Zhang, Z. Zhang, Combust. Flame 109 (1) (1997) 237-52.

[11]. R. Sullivan, B. Wilde, D.R. Noble, K. Periagaram, J.M. Seitzman, T.C. Lieuwen, Proc. Combust. Inst. 34 (2) (2013) 3203-10.

[12]. J. Sidey, E. Mastorakos, R.L. Gordon, Combust. Sci. Technol. 186 (4-5) (2014) 453-65.

[13]. R.L. Gordon, A.R. Masri, S.B. Pope, G.M. Goldin, Combust. Flame 151 (3) (2007) 495-511.

[14]. CHEMKIN-PRO 15131. Reaction Design: San Diego, 2013.

[15]. G P. Smith, D M. Golden, M. Frenklach, N W. Moriarty, B. Eiteneer, M. Goldenberg, C T. Bowman, R K. Hanson, S. Song, W C J. Gardiner, V. Lissianski & Z. Qin, Nd GRI 30. http://wwwmeberkeleyedu/gri_mech/.

[16]. B. Jiang, R. Palulli, J. E. Rivera, R. L. Gordon, and M. Talei, 20th Australasian Fluid Mechanics Conference (AFMC), Perth. (2016) 8–11.

[17]. W.S. Cleveland. J Am Stat Assoc. 74 (368) (1979) 829-836.

[18]. L.J. Spadaccini, M.B. Colket, Prog. Energy Combust. Sci. 20 (5) (1994) 431-60.

[19]. L. H. Coweli, A. H. Lefebvre. SAE Technical Paper, No. 860068. (1986).

[20]. P.R. Medwell, P.A.M. Kalt, B.B. Dally, Combust. Flame 148 (1) (2007) 48-61.

[21]. C.K. Law, C.J. Sung, Prog. Energy Combust. Sci. 26 (4) (2000) 459-505.